1 **CARBON NANOTUBE MODIFIED GLASSY CARBON ELECTRODE FOR**

2 **ELECTROCHEMICAL OXIDATION OF ALKYLPHENOL ETHOXYLATE**

3 ***Short tittle: ELECTROCHEMICAL OXIDATION OF ALKYLPHENOL***
4 ***ETHOXYLATE BY CARBON NANOTUBEs***

5 Yolanda Patiño[a], Eva Díaz[a], María Jesús Lobo-Castañón[b], Salvador Ordóñez[a]

6 *[a]Department of Chemical and Environmental Engineering,*

7 *[b]Department of Physical and Analytical Chemistry*

8 *University of Oviedo, Faculty of Chemistry, Julián Clavería s/n, 33006 Oviedo, Spain*

9 *E-mail:* diazfeva@uniovi.es

10 **Abstract**

11 The electrochemical oxidation of an emerging pollutant, 2-(4-methylphenoxy)ethanol (MPET),

12 from water has been studied by cyclic voltammetry (CV). Multiwall carbon nanotubes glassy

13 carbon electrodes (MWCNT-GCE) were used as working electrode due to their extraordinary

14 electrochemical properties.

15 The oxidation process resulted irreversible, as just a single oxidation peak was obtained, and any

16 reduction peaks was observed in the reverse scan. The electrocatalytic effect of MWCNT-GCE

17 was confirmed since the oxidation peak increases in comparison to bare-GCE. The effect of

18 functional groups on MWCNT was also studied with MWCNT-NH_2-GCE and MWCNT-COOH-GCE

19 as working electrodes. The oxidation peak current follows the order MWCNT> MWCNT-NH_2>

20 MWCNT-COOH. Taking into account the normalized peak current (I_p/A), MWCNT-NH_2 exhibits

21 the best results due its strong interaction with MPET.

22 Under optimal conditions (pH=5.0 and V_{MWCNT}=10 µL), the degradation was studied for MWCNT-

23 GCE and MWCNT-NH_2-GCE. A complete removal was obtained using MWCNT-GCE, for a

24 volume/area (V/A) ratio equal to 19 after four CV cycles. In the case of MWCNT-NH_2-GCE, the

25 maximum degradation was around 90% for V/A=37, higher than the obtained for MWCNT-GCE

26 at the same conditions. In both cases, no organic by-products were detected, being the final

27 total organic carbon removal close to 100 %.

28

29 **Keywords:** AOPs; cyclic voltammetry; emerging pollutants; endocrine disruptors

30

Introduction

Alkylphenol ethoxylates (APEs) are the main components of non-ionic surfactants, used to formulate products such as detergents, paints, plastic antioxidants, pesticides, wetting products, and petroleum recovery chemicals (Kuramitz et al., 2002), and considered an emerging organic pollutants group, with probed endocrine disrupting activity (Murray et al., 2017). Their extensive use in industrial and commercial formulations has resulted in an increase of their presence as common environmental pollutants found in sewage sludge and sediments, wastewater, surface waters, and even treated drinking (Kim et al., 2005; Nagarnaik et al., 2011). Besides, the degradation of this kind of pollutants in sewage treatment plants leads to the formation of more toxic and resistant metabolites, responsible for feminization and carcinogenesis on different organisms (Shao et al., 2003).

The European legislation by the Water Framework Directive 2000/60/EC includes some APEs in its priority list (European Commission, 2001). In addition, the European Directive No. 2003/53/EC has forbidden the use of nonylphenol and its ethoxylates in the European Union, but some industrial applications cannot replace them by alternative chemicals due to technical and economic reasons and continue using these compounds (Karci et al., 2014). Therefore, efficient methods for their removal must be developed.

Conventional treatments of water and effluents present difficulties to degrade APEs (Catapane et al., 2013) Thus, new technologies have been developed, such as advanced oxidation process (AOPs) and electrochemical degradation (Kuramitz et al., 2002; Kim et al., 2005). AOPs includes techniques like ozonation, photocatalysis, and Fenton, which employ a highly reactive oxidizing agent, such as hydroxyl radicals (HO·). Although AOPs are a good alternative and they are widely studied, they present some disadvantages: expensive process, excess consumption of chemicals and, in many cases, production of by-products of unknown effects, even more harmful than the starting products.

On the other hand, although the electrochemical degradation has been studied at lower extent than the abovementioned techniques, it presents several advantages, such as easiness of operation, the utilization of mild temperatures and pressures. At the same time, if the pollutant is oxidized, it can produce a complete mineralization of the target compound (Kim et al., 2005). All these facts make this technique as a good alternative for APEs degradation.

It is also necessary to take into account that these compounds are present in water at very low concentration, in the order of $\mu g \cdot L^{-1}$ to $ng \cdot L^{-1}$, which is a disadvantage for their removal (Esteban

63 et al., 2014), although the concentration can be increased through adsorption/desorption cycles

64 (Patiño et al., 2017a).

65 Although the degradation should be carried out at constant potential, the application of a sweep

66 potential is important in order to characterize the reaction and to obtain the best configuration

67 for the different experimental variables. In this way cyclic voltammetry (CV) is commonly used

68 to characterize redox systems, as well as to obtain information about the electrode transfer

69 kinetics. Besides, CV has the advantage that with scanning the potential in both directions, it

70 provides the opportunity to explore the electrochemical behaviour of species generated at the

71 electrode (Settle et al., 1997).

72 Regarding to the working electrode, the electrochemical degradation can be improved with

73 modified electrodes, which allow accelerating electron transfer for the electrochemical

74 oxidation. Recently, multiwall carbon nanotube (MWCNT) are proposed for modifying

75 electrodes due to their appropriate features - high surface area and porosity, enhanced

76 electronic properties and rapid electrode kinetics – (Moyo et al., 2013). Besides, functionalized

77 MWCNT can improve dispersion and generate chemical modifications on the electrode surface

78 that can favour the degradation of certain species. The electrochemical degradation of nalidixic

79 acid was studied in a previous work with non-functionalized and functionalized MWCNT-GCE

80 (MWCNT-NH$_2$ and MWCNT-COOH) as working electrodes (Patiño et al., 2017b). The nalidixic acid

81 was completely reduced to less toxic compounds using MWCNT-GCE as working electrode,

82 which demonstrate the effectiveness of this technique. However, it is necessary to extend the

83 study to other compounds with different electrochemical active functional groups to extend the

84 effectiveness of electrochemical degradation.

85 For this reason, in this work, the electrochemical oxidation of 2-(4-methylphenoxy)ethanol,

86 MPET, as representative of APEs has been studied by CV at MWCNT modified glassy carbon

87 electrodes (MWCNT-GCE), and the influence of several variables such as pH, scan rate and

88 amount of MWCNT have been studied. In order to determine the effect of functional groups on

89 MWCNT, the electrochemical behaviour under two functionalized MWCNT – MWCNT-NH$_2$ and

90 MWCNT-COOH – was compared with MWCNT under optimal conditions. In this way, the best

91 working electrode for a complete degradation of MPET by a green technology could be selected.

92

93 **Materials and Methods**

94 *Chemicals and reagents*

95 2-(4-methylphenoxy)ethanol (MPET) was purchased from TCI Europe N.V., with a purity > 98%

96 and used in the experiments directly without any further purification.

97 The chemicals employed for the phosphate buffer (PBS) (NaCl, KCl, KH_2PO_4 and Na_2HPO_4),

98 $K_4[Fe(CN)_6]$ and $K_3[Fe(CN)_6]$ were obtained from Sigma-Aldrich.

99 Three different commercial multi-walled carbon nanotubes manufactures by Dropsense

100 (MWCNT, MWCNT-NH_2 and MWCNT-COOH) were tested in this work.

101

102   *Instrumentation*

103 Cyclic voltammetry, were performed using a Zahner XPOT Potentiostat. The surface areas of the

104 working electrodes were performed using a μ-Autolab Potentiostat/Galvanostat PGSTAT20.

105 Batch oxidation was performed in an undivided electrolytic cell with a conventional three

106 electrodes arrangement: bare or modified glassy carbon (GCE) as working electrode, saturated

107 calomel (SCE) as reference electrode and platinum (Pt) as auxiliary electrode. Before each

108 measure, the solution was deoxygenated by passing purified nitrogen gas for 20 min, which

109 prevents any interference from oxygen signals. Besides, prior to each analysis a blank was

110 performed analyzing the buffer without MPET, to ensure that once the compound was added,

111 the response obtained was only relative to MPET.

112 MPET and the by-products obtained after electrochemical degradation were quantified by

113 GC-MS in a Shimadzu GC/MS QP2010 Plus instrument, using a 30 m long TRB-5MS capillary

114 column by prior extraction in chloroform using a volume ratio (1:1) which allows to determine

115 concentrations of order of ppb. Likewise, the MPET degradation was confirmed by total organic

116 carbon (TOC) measurements, which were performed using a TOC analyser (Shimadzu TOC-

117 VCSH).

118

119   *Preparation of the modified electrodes*

120 Suspensions of MWCNTs were prepared by dispersing into dimethylformamide (DMF)

121 (0.25 g·L^{-1}) using ultrasonication until obtain a well-dispersed suspension (García-González et al.,

122 2013).

123 The bare-GCE was polished successively with 0.3 and 0.05 μm alumina slurries, and washed by

124 ultrasonication in double distilled deionized water. After the electrode was dried in the air, it

125 was dropped by depositing 5, 10 or 15 μL of the MWCNTs suspension on the working area and

126 then dried under room temperature before electrochemical measurements.

127

128   **Results and Discussion**

129   *Surface area electrode study*

130   Before starting the experiments, it is necessary to determine the active surface areas. They were

131   obtained by cyclic voltammetry (CV) using 1mM $K_3[Fe(CN)_6]$ solution in PBS buffer at different

132   scan rates. According to Randles-Sevcik equation, which relates the peak current (I_p) to scan rate

133   potential (v) at 20°C for an electrochemically reversible process (Eq. 1)

134

135    $$i_p = 2.69 \times 10^5 \, n^{3/2} \, A \, C_0 \, D_R^{1/2} \, v^{1/2}$$ (1)

136

137   Where i_p is the peak current, n is the number of electron transfer (n=1), A is the surface area of

138   the electrode, C_0 is the concentration of species being oxidised, D_R is the diffusion coefficient

139   (D_R= 7.6 x 10^{-6} cm^2s^{-1}) and v is the scan rate; the electrochemically active area can be estimated

140   from the slope of i_p vs $v^{1/2}$.

141   The electrode surface areas obtained follow the order: MWCNT (0.135 cm^2) > MWCNT-NH$_2$

142   (0.054 cm^2) > MWCNT-COOH (0.051 cm^2) > Bare (0.040cm^2).

143   The electrochemical effective surface area increases after modification of GCE. This increase is

144   less pronounced for MWCNT-COOH and MWCNT-NH$_2$. However, for MWCNT the effective

145   surface area increases more than three times compared with the bare electrode, and more than

146   twice for functionalized MWCNT. These differences were attributed in a previous work (Patiño

147   et al., 2017b) to the more uniform surface with several carbon nanotubes layers and high film

148   thickness (0.9 μm) of the MWCNT, whereas functionalized materials present lower density of

149   carbon nanotubes.

150   There is also consensus in the literature about the modification of the electrode surface area

151   after the deposition of the carbon nanotubes, being in all cases the final area after modification

152   higher than for bare-GCE (d et al., 2011; Dogan-Topal et al., 2013).

153

154   *Electrochemical behaviour of MPET on GCE and MWCNT modified electrode*

155   The cyclic voltammogram of 1·10^{-5} M MPET on bare-GCE and MWCNT-GCE at pH 5 in PBS buffer

156   solution is shown in Fig. 1. As can be seen in the figure, the oxidation process of MPET was

157   irreversible for both electrodes, since no peak was observed in the reverse scan. Oxidation peaks

158   were observed at 1.28 and 1.31, for bare-GCE and MWCNT-GCE, respectively. It is observed that

159   the peak current increases at MWCNT-GCE which may be indicative of the catalytic effect of

160   MWCNT on the electrochemical oxidation of MPET (Jain and Rather, 2011; Jain and Sharma,

161   2012). The reason of this improvement with MWCNT is usually attributed to their electronic

162   structure and the higher effective area of the electrode. Taking into account the density current

163   (peak current/electrode area), the maximum value is also obtained for MWCNT, indicating that

164   the effective surface area is not the only parameter determining the electrochemical response

165   (Fig. 1b). The high electrical conductivity of carbon nanotubes accelerates the electron transfer

166   reaction rate in the oxidation process (Gupta et al., 2013). Similar behaviour was also observed

167   by other authors using multiwall carbon nanotubes modified glassy carbon electrode as working

168   electrode (Fotouhi and Alahyari, 2010; Gupta et al., 2013).

169   Once the influence of MWCNT on the MPET oxidation was demonstrated, it is important to

170   determine the optimum amount of MWCNT to drop on the electrode, since it can modify the

171   properties and functions of the surface electrode. For this reason, different volumes – 5, 10 and

172   15 µL – of the MWCNT suspension were dropped, and the peak current was compared (Fig.2).

173   The oxidation peak current increases with increases in the amount of MWCNT up to 10 µL,

174   volume from which the peak current decreases. The peak current variation is related to the

175   thickness of the film. If the film is too thin, the amount of MPET adsorbed on the electrode

176   surface is small, which involves a small peak current. Contrary, when it is too thick, film

177   conductivity gets reduced, making the film less stable and MWCNTs could leave off the electrode

178   surface easily (Jain and Rather, 2011; Patil et al., 2011). Besides, the thick electrode hinders the

179   conductivity through the whole film, decreasing in this way the ability of the molecule to be

180   adsorbed and, hence, to be degraded what is showed in a slower peak current (Fotouhi and

181   Alahyari, 2010; Jain and Sharma, 2012; Dogan-Topal et al., 2013). Therefore, 10 µL was selected

182   as the optimum amount of MWCNT suspension.

183   The effect of the concentration on the voltammogram is shown in Fig. 3, where the peak current

184   obtained using MWCNT-GCE increases with MPET concentration. Although the response is close

185   to linearity, it cannot be considered linear with a correlation coefficient of r^2=0.9784.

186

187   *Optimization of parameters*

188   Cyclic voltammograms on MWCNT-GCE of $1·10^{-5}$ M MPET at different scan rates of 10 to

189   50 mVs^{-1} were done in order to investigate the effect of this parameter. By increasing the scan

190   rate, the peak current increases and also, peak potential shifted toward more positive values,

191   typical effect with increasing scan rate (Fotouhi and Alahyari, 2010; Patil et al., 2011; Dogan-

192   Topal et al., 2013).

193   Scan rate studies provide information about whether the process is controlled by diffusion or

194   adsorption. It was found that the logarithm of peak current is linear to the logarithm of scan

195   rate, according to the equation (2). If the slope is 0.5, the process is under diffusion controlled,

196   but contrary, when the slope is 1.0, the process is controlled by (Dogan-Topal et al., 2013). In

197   this case, the slope has an intermediate value, which suggests a mixed control: diffusion-

198   adsorption (Grosser, 1993).

199

200    $\ln I_p = 0.7608 \ln v + 0.387$ ($r^2 = 0.991$)   (2)

201

202   A positive shift in Ep was also observed with increase in scan rate, which confirms the irreversible

203   nature of the catalytic oxidation of MPET (Moyo et al., 2013). Likewise, the electrochemical

204   behaviour is also affected by the pH of the supporting electrolyte. The voltammetric oxidation

205   of MPET was studied in the pH range of 3 to 9. As shown in Fig. 4 the oxidation peak current

206   reaches a maximum in current at pH 5, after that it decreases. Considering this pH effect, pH of

207   5 was chosen for the rest of experiments.

208   The relationship between the oxidation potential and pH is also represented in Fig. 4. It was

209   found that the peak potential shifted towards negative potentials with increasing pH, which

210   indicates that protons are directly involved in the oxidation of MPET (Zheng et al., 2012). The

211   oxidation peak potential increases linearly with the pH, and the linear regression equation is:

212

213   E_p (V) = 0.0515 pH + 1.5865 ($r^2 = 0.995$)   (3)

214

215   The slope is close to the theoretical Nernstian value (0.059 V), indicating the participation of the

216   same protons and electrons during the oxidation reaction (Łuczak, 2008).

217

218   *Effect of functional groups of MWCNT*

219   The effect of the functionalization of MWCNT on the electrochemical oxidation of MPET, has

220   been studied by CV using three different modified MWCNT-GCE as working electrodes: MWCNT,

221   MWCNT-NH$_2$ and MWCNT-COOH. The behaviour is different for each working electrode, which

222   can be seen from Fig. 5. The peak current increases in the order: MWCNT > MWCNT-NH$_2$ >

223   MWCNT-COOH, coincident with the increase in the electrode surface area (Fig 5a). However in

224   the case of functionalized MWCNT, where the effective area is very similar, there are major

225   differences in the peak intensity obtained, suggesting that other factor influences the oxidation

226   process. It was demonstrated that the process presents mixed control: diffusion-adsorption.

227   During the electrochemical process, MPET is adsorbed on the electrode surface, where the

228   electrochemical oxidation takes places, so the peak current trend may be affected also by the

229   different strength of the adsorption due to the functionalization of MWCNT. The adsorption of

230   MPET onto MWCNT and functionalized MWCNT was studied in a previous work, by batch

231   adsorption at three different temperatures (298, 303 and 308 K) (Patiño et al., 2015). The

232   strength of the interaction was measured in terms of standard enthalpy ($\Delta H°$, kJ·mol^{-1}) and

233   follows the order MWCNT-NH$_2$ (101.7) > MWCNT (88.1) > MWCNT-COOH (67.4). In order to take

234   into account the differences in active area of the selected electrodes, and with the aim to

235   determine if the adsorption influences the electrochemical oxidation, the density current (I_p/A,

236   measured in µA/cm^2) has been calculated and its evolution with the pH represented (Fig. 5b).

237   The density current decreases in the order: MWCNT-NH$_2$ > MWCNT > MWCNT-COOH, which is

238   coincident with the strength of the interaction (Patiño et al., 2015) (Fig. 6). As the strength of

239   interaction increases, the stability of the MPET adsorbed increases, decreasing the trend to leave

240   the electrode surface. Thus, a higher strength implies a higher normalized peak current.

241   Besides, MWCNT-NH$_2$ presents the highest normalized peak current, since the nitrogen content

242   in MWCNT could increase its affinity for MPET. In this case, the electronic interactions play a key

243   role, where the nitrogen present on the MWCNT acts as electron donor and the aromatic ring

244   of MPET as electron receptor, promoting the adsorption of the pollutant on the electrode

245   surface (Fan et al., 2011; Patiño et al., 2015).

246   On the contrary, there is no a relationship regarding to the effect of the surface chemistry. The

247   electrode surface is negatively charged, since working at pH=5, it is in all cases higher than the

248   pH$_{PZC}$ of the multiwall carbon nanotubes - pH$_{PZC}$ (MWCNT)=4.19, pH$_{PZC}$ (MWCNT-NH2)=4.70 and

249   pH$_{PZC}$ (MWCNT-COOH)=0.64 – (Patiño et al., 2015). On the other hand, MPET is expected to be

250   in the protonated form (pKa≈14), acquiring positive charge. Therefore, MWCNT-COOH should

251   present the best behaviour if the effect of the surface chemistry plays an important role, since

252   it presents the most negative surface (pH$_{PZC}$=0.64), which is contrary to the results obtained

253   (Patiño et al., 2015).

254

255   *Removal of MPET using MWCNT-GCE and MWCNT-NH$_2$-GCE electrodes*

256   MPET degradation has been studied by CV using two different working electrodes. Although

257   MWCNT-NH$_2$ presents the highest density current, it must be taken into account that many

258   times the electrode surface is a limiting factor. Therefore both, the effect of area and strength

259   of interaction, should be considered. For this reason, MWCNT and MWCNT-NH$_2$ modified GCE

260   have been tested as electrodes.

261   Both working electrodes were tested by CV using a potential range of 0.9 to 1.7 V for an initial

262   concentration of 1·10^{-5} M. The final concentration and possible intermediates were analysed by

263   GC-MS with the aim to estimate the percentage of degradation.

264   The surface area of the electrodes is a constant parameter after modification, so it is necessary

265   to obtain the total volume to be treated for which the maximum degradation is obtained. In this

266   way, the optimum volume/area (V/A) ratio will be obtained.

267   The oxidation of MPET was carried out initially in a total volume of 5 mL for both working

268   electrodes: MWCNT (V/A=37) and MWCNT-NH$_2$ (V/A=98) modified GCE. After one CV, the

269   degradation of MPET was lower than 31% for both working electrodes, so several cycles of CV

270   were performed in order to degrade a new fraction of the pollutant at each new cycle, increasing

271   the percentage of degradation (Fig. 7 empty symbols). With each new CV cycle, a new amount

272   of MPET is adsorbed on the electrode surface and therefore oxidized on the electrode surface.

273   The maximum degradation obtained was 79 and 58% for MWCNT and MWCNT-NH$_2$ respectively

274   (between 2.6 and 2.8 times greater than for one CV), keeping it constant after four CV cycles.

275   Since it is not possible to increase the MPET degradation by more CV cycles, the next strategy

276   proposed to get this purpose was to decrease the total volume to be treated. In this way, the

277   volume/area (V/A) ratio was modified in order to obtain a higher degradation (Fig. 7 full

278   symbols). For MWCNT modified GCE, the degradation was carried out for a total volume of 2.5

279   mL (V/A=19) and for one to five cyclic voltammograms. In this case, the degradation obtained

280   after one CV is more than double compared to a total volume of 5 mL, and a total degradation

281   was achieved after four CV. In the case of MWCNT-NH$_2$ modified GCE, the total volume was

282   decreased to 1.9 mL (V/A=37.3), because it is the smallest volume that supports the

283   experimental device and it is coincident with the first V/A ratio employed for MWCNT. In this

284   case the maximum degradation is around 85 - 90% and more or less constant after three CV. For

285   this working electrode it was no possible to reach a complete degradation due to the

286   experimental constraints.

287   When the V/A ratio is the same for both electrodes, the degradation is a bit higher for MWCNT-

288   NH$_2$-GCE than for MWCNT-GCE, which is due to the high interaction strength. The MPET

289   adsorbed on the electrode surface is more stable in this case, making it more difficult to leave

290   the electrode surface during the degradation process. However, when the volume to be treated

291   is a limiting factor, MWCNT-GCE provides better results. The results provide a new pathway for

292   the electrochemical degradation of these kind of pollutants and the degradation can be

293   performed at constant potential, higher than the peak potential (1.31 V). Kuramitz et al. (2002)

294   studied the electrochemical removal of p-nonylphenol at constant potential with a carbon fibre

295   electrode as working electrode with a removal efficiency of 100%. Besides, the results obtained

296   by electrochemical degradation, can be compared with those obtained by other authors using

297   advanced oxidation processes (AOPs). Nagarnaik et al. (2011) studied the degradation of APEs

298 by UH − UV/H$_2$O$_2$, FH − Fe/H$_2$O$_2$, UFH − Fe/UV/H$_2$O$_2$. The maximum removal efficiency follows

299 the order: UH − UV/H$_2$O$_2$ (97.1%) > UFH − Fe/UV/H$_2$O$_2$ (85.8%) > FH − Fe/H$_2$O$_2$ (95.5%) with values

300 lower or similar than the obtained in the present work. Karci et al. (2014) studied the oxidation

301 of an nonionic surfactant (NP-10) by three AOPs, whose oxidation efficiency decreases in the

302 order: UV/H$_2$O$_2$ (100%) > Photo-Fenton (100%) > Fenton (20%). Although in some cases, a total

303 oxidation could be obtained by AOPs, electrochemical oxidation provides a low cost and clean

304 technology.

305 The final concentration and sub-products formation was analysed by GC-MS after each test,

306 observing an important diminution of the MPET after the electrochemical degradation, which

307 confirms that oxidation takes place. Likewise, any other compound was detected, which

308 suggests that MPET is completely removed from the aqueous sample. In order to confirm the

309 absence of MPET and other organic compounds in the final solution, Fig. 8 shows the evolution

310 of the total organic carbon (TOC) with each new cycle. The analysis were carried out for MWCNT

311 and MWCNT-NH$_2$ under conditions where maximum degradation was reached. TOC removal

312 reaches values of which also confirms the best behaviour of MWCNT for MPET degradation.

313

314   **Conclusions**

315 The results obtained offer an alternative for the degradation of MPET from water by cyclic

316 voltammetry.

317 MWCNT modified GCE exhibits an electrocatalytic effect on the electrochemical oxidation of

318 MPET, with a peak intensity four times higher than bare-GCE.

319 Different parameters were optimized in order to obtain an improved oxidation: carbon

320 nanotube loading (10 µL of CNTs suspension), the pH (5.0) and the scan rate (50 mV·s^{-1}).

321 Functionalized MWCNT were checked in order to determine how the functional groups on

322 MWCNT affect to the electrochemical oxidation process. The peak current (Ip) increases in the

323 order: MWCNT > MWCNT-NH$_2$ > MWCNT-COOH, coincident with the electrode surface area. The

324 order for the density current (I$_p$/A) changes: MWCNT-NH$_2$ > MWCNT > MWCNT-COOH. This

325 trend is coincident with the strength of adsorption on the electrode surface and in addition, the

326 nitrogen presents on MWCNT-NH$_2$ increases the affinity for MPET through electronic

327 interaction.

328 The MPET was removed with MWCNT-GCE after four CV cycles under optimal conditions and

329 V/A ratio equal to 19. In the case of MWCNT-NH$_2$ the maximum degradation obtained was

330 around 90% for a V/A = 37. Degradation was confirmed by TOC measurements, reaching a

331 reduction between 93 and 99 % after the four CV cycles, as well as by GC-MS analysis of the

332 treated samples, where no by-products were observed. Therefore, the MPET adsorbed on the
333 electrode surface in each CV cycle is oxidized, allowing a new amount of compound to be
334 deposited and oxidized. This way provides a green methodology without producing more toxic
335 compounds.

336
337

343
344

345 **References**

346 Catapane M., Nicolucci,C., Menale C., Mita L., Rossi S., Mita D.G. & Diano, N. 2013 Enzymatic
347 removal of estrogenic activity of nonylphenol and octylphenol aqueous solutions by immobilized
348 laccase from Trametes versicolor. *J. Hazard Mat*. **248–249**, 337-346.

349 Dogan-Topal B., Bozal-Palabıyık B., Uslu B. & Ozkan S.A. 2013 Multi-walled carbon nanotube
350 modified glassy carbon electrode as a voltammetric nanosensor for the sensitive determination
351 of anti-viral drug valganciclovir in pharmaceuticals. *Sens. Actuators B: Chem*. **177**, 841-847.

352 European Commision, Decision No. 2455/2001/EC of the European Parliament and of the
353 Council of 20 November 2001 establishing the list of priority substances in the field of water
354 policy and amending Directive 2000/60/EC, Official Journal of the EC, L331, 15.12.2001

355 Esteban S., Gorga M., Petrovic M., González-Alonso S., Barceló D. & Valcárcel Y. , 2014 Analysis
356 and occurrence of endocrine-disrupting compounds and estrogenic activity in the surface waters
357 of Central Spain. *Sci. Total Environ*. **466–467**, 939-951.

358 Fan J., Yang W. & Li A. 2011 Adsorption of phenol, bisphenol A and nonylphenol ethoxylates
359 onto hypercrosslinked and aminated adsorbents. *React. Funct. Polym*. **71**(10), 994-1000.

360 Fotouhi L. & Alahyari M. 2010 Electrochemical behavior and analytical application of
361 ciprofloxacin using a multi-walled nanotube composite film-glassy carbon electrode. *Colloids*
362 *Surf. B: Biointerfaces* **81** (1), 110-114.

363 García-González R., Fernández-La Villa A., Costa-García A. & Fernández-Abedul M.T. 2013
364 Dispersion studies of carboxyl, amine and thiol-functionalized carbon nanotubes for improving
365 the electrochemical behavior of screen printed electrodes. *Sens. Actuators B: Chemical* **181**, 353-
366 360.

367 Gupta V.K., Jain A.K. & Shoora S.K. 2013 Multiwall carbon nanotube modified glassy carbon
368 electrode as voltammetric sensor for the simultaneous determination of ascorbic acid and
369 caffeine. *Electrochim. Acta* **93**, 248-253.

370 Jain R. & Rather J.A. 2011 Voltammetric determination of antibacterial drug gemifloxacin in
371 solubilized systems at multi-walled carbon nanotubes modified glassy carbon electrode. *Colloids*
372 *Surf. B: Biointerfaces* **83** (2), 340-346.

373 Jain R. & Sharma S. 2012 Glassy carbon electrode modified with multi-walled carbon nanotubes
374 sensor for the quantification of antihistamine drug pheniramine in solubilized systems. *J. Pharm.*
375 *Anal*. **2** (1), 56-61.

376 Gosser Jr D.K. 1993. Cyclic Voltammetry, Simulation and Analysis of Reaction Mechanisms, New
377 York.

378 Karci A., Arslan-Alaton I., Bekbolet M., Ozhan G. & Alpertunga B. 2014 H_2O_2/UV-C and Photo-
379 Fenton treatment of a nonylphenol polyethoxylate in synthetic freshwater: Follow-up of
380 degradation products, acute toxicity and genotoxicity. *Chem. Eng. J*. **241**, 43-51.

381 Kim J., Korshin G.V. & Velichenko A.B. 2005 Comparative study of electrochemical degradation
382 and ozonation of nonylphenol. *Water Res*. **39** (12), 2527-2534.

383 Kuramitz H., Saitoh J., Hattori T. & Tanaka S. 2002 Electrochemical removal of p- nonylphenol
384 from dilute solutions using a carbon fiber anode. *Water Res*. **36** (13), 3323-3329.

385 Łuczak T. 2008 Preparation and characterization of the dopamine film electrochemically
386 deposited on a gold template and its applications for dopamine sensing in aqueous solution.
387 *Electrochim. Acta* **53** (19), 5725-5731.

388 Moyo M., Okonkwo J.O. & Agyei N.M. 2013 A Novel Hydrogen Peroxide Biosensor Based on
389 Adsorption of Horseradish Peroxidase onto a Nanobiomaterial Composite Modified Glassy
390 Carbon Electrode. *Electroanalysis* **25** (8), 1946-1954.

391 Murray A., Örmeci B. & Lai E.P.C. 2017 Use of sub-micron sized resin particles for removal of
392 endocrine disrupting compounds and pharmaceuticals from water and wastewater. *J. Environm.*
393 *Sci*. **51**, 256-264.

394 Nagarnaik P.M. & Boulanger B., 2011 Advanced oxidation of alkylphenol ethoxylates in aqueous
395 systems. *Chemosphere* **85** (5), 854-860.

396 Patil R.H., Hegde R.N. & Nandibewoor S.T. 2011 Electro-oxidation and determination of
397 antihistamine drug, cetirizine dihydrochloride at glassy carbon electrode modified with multi-
398 walled carbon nanotubes*. Colloids Surf. B: Biointerfaces* **83** (1), 133-138.

399 Patiño Y., Díaz E., Ordóñez S., Gallegos-Suarez E., Guerrero-Ruiz A. & Rodríguez-Ramos I. 2015
400 Adsorption of emerging pollutants on functionalized multiwall carbon nanotubes. *Chemosphere*
401 **136**, 174-180.

402 Patiño Y., Díaz E. & Ordóñez S. 2017a Micropollutants pre-concentration using adsorption–
403 desorption cycles: application to chlorinated paraffins and alkyl-phenol derivatives. *J. Chem.*
404 *Technol. Biotechnol.* **92** (5), 1076-1084.

405 Patiño Y., Pilehvar S., Díaz E., Ordóñez S. & De Wael K. 2017b Electrochemical reduction of
406 nalidixic acid at glassy carbon electrode modified with multi-walled carbon nanotubes. *J Hazard*
407 *Mat*. **323**, 621-631.

408 Settle F.A. 1997. Handbook of instrumental techniques for analytical chemistry. Upper Saddle
409 River, NJ : Prentice Hall PTR.

410 Shao B., Hu J., & Yang M. 2003 Nonylphenol Ethoxylates and Their Biodegradation Intermediates
411 in Water and Sludge of a Sewage Treatment Plant. Bull Environ. *Contam. Toxicol*. **70** (3), 0527-
412 0532.

413 Zheng Q., Yang P., Xu H., Liu J. & Jin L. 2012 A simple and sensitive method for the determination
414 of 4-n-octylphenol based on multi-walled carbon nanotubes modified glassy carbon electrode.
415 *J. Environ. Sci.* **24** (9), 1717-1722.

416

418 **FIGURE CAPTIONS**

419

420

421

422 **Figure 1.** Electrochemical oxidation of 1×10^{-5} M MPET (CV, scan rate 50 mVs^{-1}) over
423 the bare GCE electrode (- - -), and MWCNT-GCE (—). Background electrolyte signal is
424 also displayed (....), represented as peak current *vs* potential (SCE) (a) and density
425 current *vs* potential (SCE) (b).

426 **Figure 2.** Effect of accumulation volumes of MWCNT on peak current response of
427 $1 \cdot 10^{-5}$ M MPET.

428 **Figure 3.** Voltammograms obtained with MWCNT-GCE (CV, scan rate 50 mVs^{-1}) for
429 different MPET concentration: (a) $1 \cdot 10^{-5}$, (b) $3 \cdot 10^{-5}$, (c) $6 \cdot 10^{-5}$, (d) $9 \cdot 10^{-5}$ and (e) $1.2 \cdot 10^{-4}$.
430 Represented as peak current *vs* potential (SCE).

431 **Figure 4.** Dependence of oxidation peak current (•) and oxidation peak potential (□), as
432 a function of pH by cyclic voltammetry on MWCNT-GCE (1×10^{-5} M MPET and scan rate:
433 50 mVs^{-1})

434 **Figure 5.** Effect of functionalized MWCNT on the electro-oxidation of MPET by CV (pH
435 5 and scan rate 50 mVs^{-1}): MWCNT-GCE (—), MWCNT-NH$_2$-GCE (---),MWCNT-COOH-
436 GCE (---) and Bare-GCE (– –) as working electrodes. Represented as peak current *vs*
437 potential (SCE) (a) and density current *vs* potential (SCE) (b)

438 **Figure 6.** Influence of the enthalpy of adsorption (kJ·mol^{-1}) in the ratio (I$_p$/A) for electro-
439 oxidation of MPET by CV under three different working electrodes: MWCNT-GCE,
440 MWCNT-NH$_2$-GCE and MWCNT-COOH-GCE (pH 5 and scan rate 50 mVs^{-1}).

441 **Figure 7.** Degradation of MPET by CV (pH 5 and scan rate 50 mVs^{-1}) under different
442 working electrodes and V/A ratio: (•) MWCNT-GCE, VT/A = 19, (○) MWCNT-GCE, VT/A
443 = 37, (□) MWCNT-NH$_2$-GCE, VT/A = 98, (■) MWCNT-NH$_2$-GCE, VT/A = 37

444 **Figure 8.** Evolution of TOC under different CV cycles for MWCT at V$_T$/A=19 (solid blue
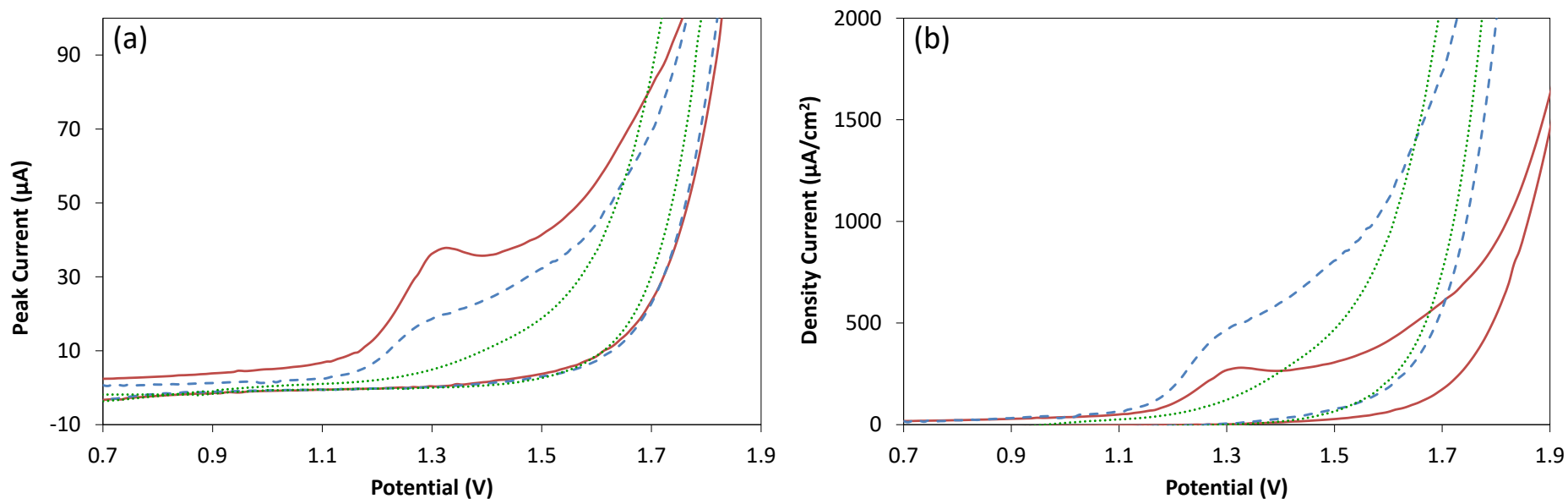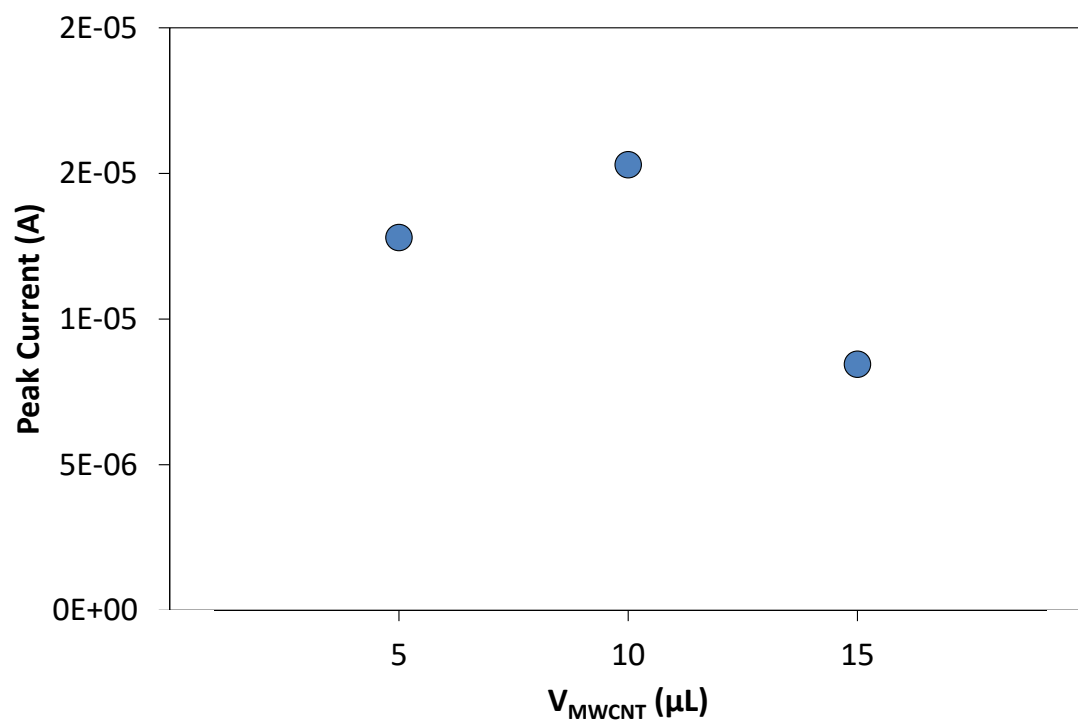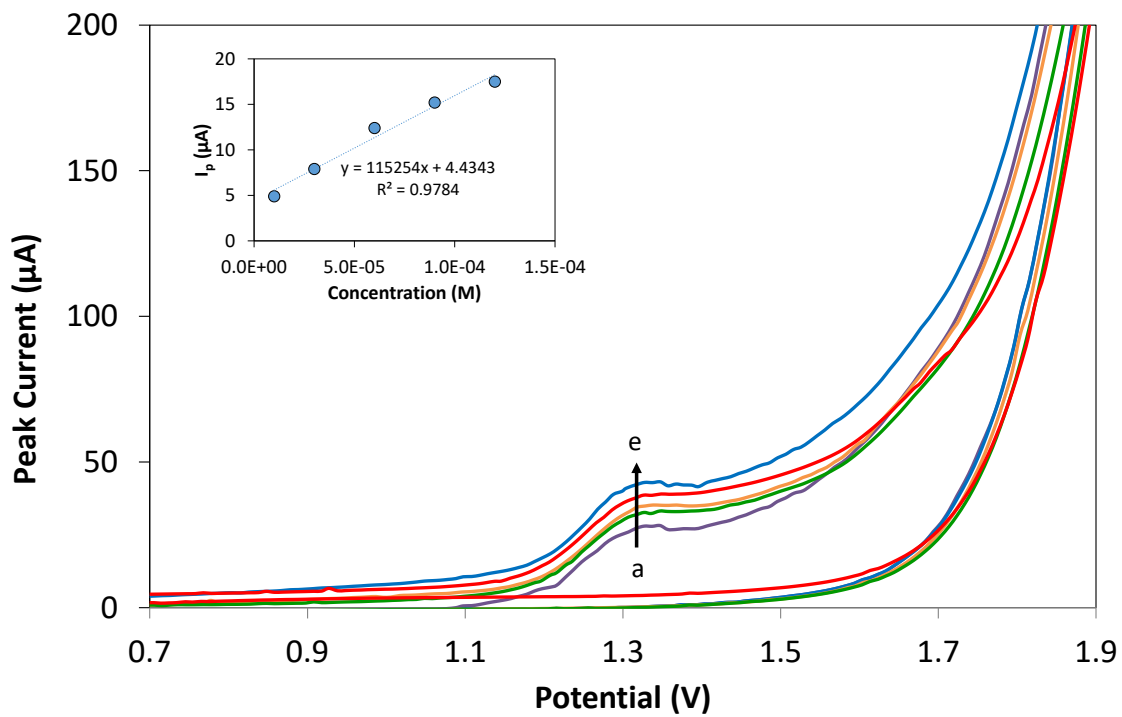445 bar) and MWCNT-NH$_2$ at V$_T$/A=37 (striped yellow bar)

446

Figure 1

Peak Current (A)

2E-05

2E-05

1E-05

5E-06

0E+00

5   10   15

V_{MWCNT} (μL)

Figure 2

Figure 3

Figure 4

Figure 5

1

2
3 **Figure 6**
4

Figure 7

Figure 8

7
8
9
10
11